Computational modelling of the right ventricle in repaired tetralogy of Fallot: can it provide insight into patient treatment?†

Benedetta Leonardi[1], Andrew M. Taylor[2]*, Tommaso Mansi[3], Ingmar Voigt[3,4], Maxime Sermesant[5], Xavier Pennec[5], Nicholas Ayache[5], Younes Boudjemline[6], and Giacomo Pongiglione[1]

[1]Bambino Gesù Children's Hospital and Research Institute, Rome, Italy; [2]UCL Institute of Cardiovascular Sciences and Great Ormond Street Hospital for Children, Great Ormond Street, London WC1N 3JH, UK; [3]Siemens Corporation, Corporate Research and Technology, Imaging and Computer Vision, Princeton, NJ, USA; [4]Pattern Recognition Lab, Friedrich-Alexander-University, Erlangen, Germany; [5]Asclepios Research Team, INRIA Sophia Antipolis, Nice, France; and [6]Université Paris Descartes, Assistance Publique des Hopitaux de Paris, Necker Hospital for Sick Children, Paris, France

Aims	Pulmonary regurgitation (PR) causes progressive right ventricle (RV) dilatation and dysfunction in repaired tetralogy of Fallot (rToF). Declining RV function is often insidious and the timing of pulmonary valve replacement remains under debate. Quantifying the pathophysiology of adverse RV remodelling due to worsening PR may help in defining the best timing for pulmonary valve replacement. Our aim was to identify whether complex three-dimensional (3D) deformations of RV shape, as assessed with computer modelling, could constitute an anatomical biomarker that correlated with clinical parameters in rToF patients.
Methods and results	We selected 38 rToF patients (aged 10–30 years) who had complete data sets and had not undergone PVR from a population of 314 consecutive patients recruited in a collaborative study of four hospitals. All patients underwent cardiovascular magnetic resonance (CMR) imaging: PR and RV end-diastolic volumes were measured. An unbiased shape analysis framework was used with principal component analysis and linear regression to correlate shape with indexed PR volume. Regurgitation severity was significantly associated with RV dilatation ($P = 0.01$) and associated with bulging of the outflow tract ($P = 0.07$) and a dilatation of the apex ($P = 0.08$).
Conclusion	In this study, we related RV shape at end-diastole to clinical metrics of PR in rToF patients. By considering the entire 3D shape, we identified a link between PR and RV dilatation, outflow tract bulging, and apical dilatation. Our study constitutes a first attempt to correlate 3D RV shape with clinical metrics in rToF, opening new ways to better quantify 3D RV change in rToF.
Keywords	Computer modelling • Right ventricle • Tetralogy of Fallot • Pulmonary regurgitation

Introduction

Early surgical repair of tetralogy of Fallot (rToF) often leaves patients with residual pulmonary regurgitation (PR), which is associated with significant late complications—exercise intolerance, right heart failure, arrhythmias, and sudden death.[1–3] Pulmonary valve replacement (PVR)[4,5] in rToF has become the treatment of choice to treat late PR, and halt or at least slow down the progression of adverse right ventricular (RV) remodelling and its sequelae. Unfortunately, PVR is not a definitive therapeutic option and clinicians have to balance the immediate benefits of PVR against the likelihood of long-term complications and the need for future re-intervention. Accurate follow-up of patients is necessary, often with a serial assessment of RV size and systolic function, using cardiovascular magnetic resonance (CMR) imaging;[6–10] however, there are no clear, evidence-based guidelines on the optimal timing for PVR.[11]

* Corresponding author. Tel: +44 20 7405 9200 (ext. 5616), Email: a.taylor76@ucl.ac.uk

Computational modelling analysis of congenital heart disease,[12] and, in particular, how RV dilatation evolves over time, could provide insights into pathological mechanisms, resulting in a useful support tool for disease evaluation and therapy planning. RV and RV outflow tract anatomy are complex and vary significantly among rToF patients[13,14] and, therefore, quantifying the entire RV shape is challenging. Recently, we have described a new method of computational modelling to analyse three-dimensional (3D) shapes and compare them with clinical features for the RV.[15] A few studies have partially analysed the 3D alterations of the RV anatomy in rToF.[16,17] Results from these studies suggest important differences in regional RV remodelling, but could not identify local changes in RV anatomy because the volume metrics used were too coarse.

In the present study, our aim was to investigate the clinical applicability of our computational modelling method. Assuming that RV shape can provide insight into the heart condition, we applied our shape analysis method to establish new quantitative metrics based on the RV shape that may assist in helping to plan when individual patients should undergo PVR. In particular, we aimed at identifying abnormal RV shape features that could reveal severe deterioration in the cardiac structure due to PR, which together with the clinical parameters may help in timing of PVR.

Methods

Subjects

As part of a collaborative study involving four hospitals (Gaslini Institute, Genoa, Italy; Great Ormond Street Hospital for Children, London, UK; Hôpital Necker—Enfants Malades, Paris, France; Bambino Gesù Children's Hospital and Research Institute, Rome, Italy); every willing, consecutive patient with rToF was recruited over a 3-year period ($n = 314$), as part of the FP6 Health-e-Child project (European project, IST-2004-027749). Local ethical approval was given by all four hospitals for the research, and informed consent was received from the patients (and/or their legal guardians) to partake in the study.

From the 314 patients enrolled into the Health-e-Child project, 49 had complete data sets that enabled them to be included in our current study (clinical features, echocardiogram, full CMR examination, and RV segmentation). These data sets were used to define a representative RV shape for the group. Subsequent analysis of shape and PR volume was carried out on the 38 patients (26 males), from these 49 who had not undergone PVR prior to CMR. The majority of these patients ($n = 35$) had had transannular surgery at their initial repair. Clinical features of these patients are reported in Table 1. Figure 1 summarizes the different steps of our analysis.

Imaging assessment

CMR exams were acquired with 1.5T MR scanners (Avanto, Siemens and Achieva, Philips). The standard approach to measure RV volume and function using cine imaging (balanced steady-state free precession sequences), with multiple short-axis slices covering entirely both ventricles acquired during breath-holding (10−15 slices; in-plane resolution: 1.1−1.7 mm^2; slice thickness: 5− mm; 25−40 phases). Manual tracking of the endocardial contours allowed the measurement of EDV, ESV, stroke volume, and RV ejection fraction. Flow quantification was performed using through-plane phase contrast velocity mapping, with a retrospectively gated, gradient echo sequence, during free

Table I **Clinical features of 38 rToF patients (mean $\pm$ standard deviation)**

38 patients with rToF	
Age	16.34 $\pm$ 4.38 year
Body surface area	1.56 $\pm$ 0.36 m^2
Pulmonary regurgitant fraction	43.32 $\pm$ 11.77%
Indexed pulmonary regurgitant volume	31.79 $\pm$ 15.73 mL/beat/m^2

respiration technique (slice thickness 8 mm, TE 2.7 ms, TR 4.7 ms, acquisition matrix 176 × 512). The pulmonary regurgitant fraction was calculated as pulmonary retrograde flow (mL/beat) × 100/pulmonary forward flow (mL/beat). Then pulmonary regurgitant volume (PRV) was indexed for BSA to give indexed PR volume (PRVi).

Surface mesh preparation

We studied the RV shape at end-diastole, when the anatomical features of the pathology are more pronounced.[16] The RV endocardium was segmented on the end-diastolic CMR cine images by fitting an anatomically accurate geometrical model.[18] In brief, RV position, orientation, scale, and boundaries in the images were determined automatically using machine-learning algorithms based on marginal space learning and probabilistic boosting tree. An expert manually adjusted the automatic fitting whenever it was necessary (Figure 2, left panel). At the end of the process, 3D meshes of the RV were available for every patient (Figure 2, mid-panel). In the subsequent text, we refer to these meshes as shapes. To avoid any bias in the statistical analyses due to patient positioning, the 3D meshes were rigidly aligned in a common co-ordinate system using a standard least-square method.[19]

RV shape representation and quantification

Right ventricles were investigated by analysing how an ideal reference shape—the template (developed from the 49 patients)—deforms in a population of shapes—here the set of RV meshes computed from the CMR data of our patients. Intuitively, if the template is deformed in such a way that it matches the RV shape of a patient, then the deformation that is applied encodes the shape information of that patient. A rigorous mathematical framework can then be employed on the non-linear deformations to analyse the shapes.[20] Although any RV shape can be taken as the reference, to avoid any bias in the analysis, it is highly recommended to use a template that is as independent as possible from the studied population and that is 'centred'—i.e. equally distant to all subjects. In this study, we estimated the template using the method proposed by Durrleman *et al.*[20] Indeed, we have demonstrated in our previous study[15] that the resulting template is robust with respect to rToF subjects and is well centred, thus constituting a suitable reference. Our computer modelling process is as follows: we start from a template (the mean shape, represented by mathematical currents[20,21]). We then compute the transformations that deform this template to the RV shapes of our patients.[21] Using these transformations, we update the template such that it minimizes the residual errors of the template-to-patient matching. We repeat these two steps iteratively until convergence. At the end of the process, we obtain an unbiased template of the RV and the related deformations. It can be observed that in such a framework, the template and the deformations are calculated simultaneously, a key requirement for a consistent shape analysis (for mathematical details,
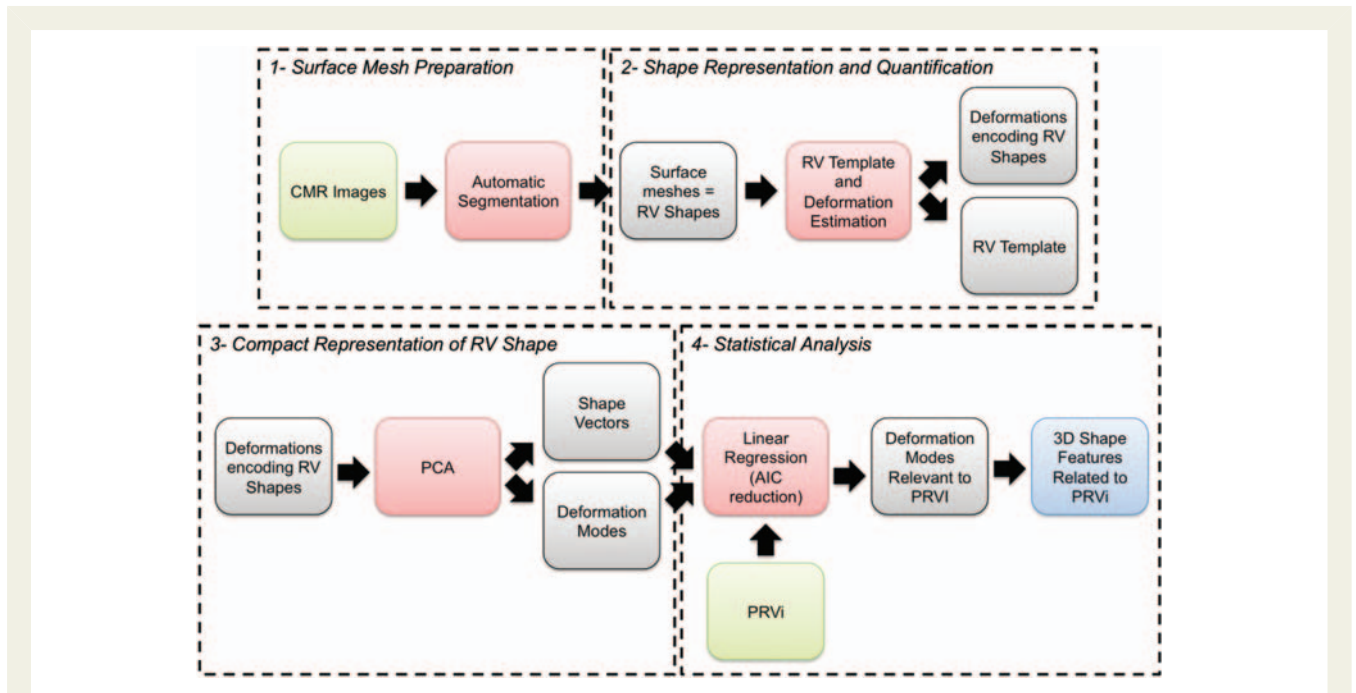
Figure 1 Analysis pipeline. The RV was first segmented from cardiac MRI. A reference template and the deformations, which mapped that template to each RV, were then computed to quantify RV shapes. PCA on deformations was performed to extract the main shape variation features and reduce model dimension. Linear regression was finally estimated to identify the shape features related to PRVi. See text for details.
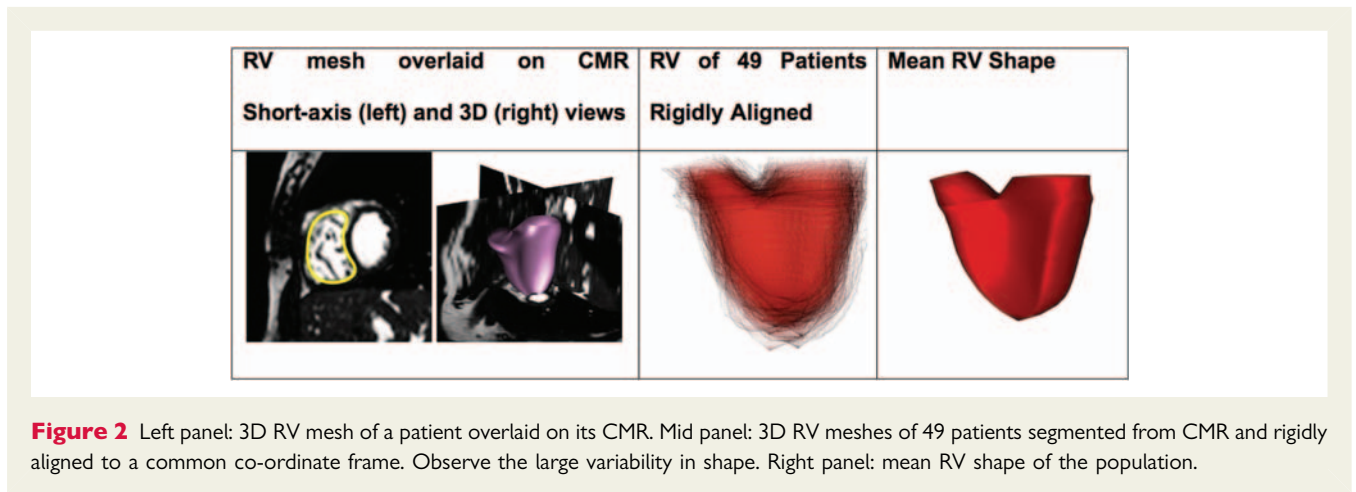

Figure 2 Left panel: 3D RV mesh of a patient overlaid on its CMR. Mid panel: 3D RV meshes of 49 patients segmented from CMR and rigidly aligned to a common co-ordinate frame. Observe the large variability in shape. Right panel: mean RV shape of the population.

see refs[15,20,21]). It should be stressed that the computed template is an ideal geometry representing the average RV observed in the population. As such, no clinical data are available for this template. In particular, this ideal RV does not come from any individual patient's CMR data, but rather represents the entire population under study.

Compact representation of patient RV shape

The non-linear deformations computed in the previous step, which encode patient RV shapes, make it possible to quantitatively correlate RV shape with clinical variables. However, direct statistics on these deformations was not possible as they were represented by too many parameters (>1000) to have a good statistical power. To

reduce the dimensionality of the problem, we thus performed a principal component analysis (PCA) of the deformations (see refs[15,20]). The 38 patients under study were used to compute the principal components of the deformations. The PCA modes, called deformation modes, represented a specific pattern of RV shape variation observed in this population (e.g. overall dilatation, apical bulging, etc.). Since this pattern is computed from the entire population, it is not related to specific clinical data or CMR images. By projecting patient deformations into the PCA space, we could represent each patient by a low-dimensional shape vector whose elements quantified the contribution of each deformation mode in patient RV shape. In other words, by definition of the PCA, the RV shape of a given patient is the weighted sum of all computed deformation modes, the weights varying from patient

to patient. As the number of elements of the shape vector was lower than the number of patients, standard statistical designs could be applied to quantitatively correlate the RV features identified by the PCA modes with clinical features.

Identification of pathological shape features

To identify shape features related to regurgitation, we related the shape vectors to PRVi using linear regression with automatic model reduction according to Akaike Information Criterion. We used indexed measurements to remove growth effects from the analysis. The idea was to estimate a reduced linear model that predicted the PRVi (measured variable) from the elements of the shape vectors (predictors). The deformation modes corresponding to the elements selected in the model encoded the 3D shape features that were related to PRVi, which we could visualize and quantify by deforming the reference template with these deformation modes. The sign of the linear regression coefficients identified the direction of correlation along the deformation mode for increasing PRVi. All the tests were performed with R (R Development Core Team, 2009). The level of significance was set at $P < 0.05$.

Results

Template of the right ventricle

Figure 2, left panel, shows a 3D RV mesh overlaid on the CMR image of a patient. *Figure 2*, mid-panel, illustrates the RV meshes of all patients aligned in a common co-ordinate system. Since the overall study was retrospective, only 49 patients out of 314 had complete CMR data. To avoid any bias, we thus computed the template using all available patients. *Figure 2*, right panel, illustrates the RV template estimated from the 49 patients. The template was well centred with respect to the population, as quantified by the standardized mean of deformations, mean/SD = 0.4 < 1). Interestingly, the patient's age that was closest to the template was 16 years whose BSA was 1.64 m². Both values were close to population average (*Table 1*), which suggests a good consistency between the template and the above-mentioned clinical features.

Relating the right ventricle shape to pulmonary regurgitation

Twenty deformation modes encoded 95% of shape variability observed in our population who had not undergone PVR ($n = 38$), resulting in 20-element shape vectors. The optimal linear model consisted of six PCA modes (*Table 2*) ($R^2 = 0.39$, $P = 0.013$). Three deformation modes were found statistically relevant to the model. Mode 1 was significantly and positively related to increasing PRVi ($P = 0.01$), while there was a positive association with Mode 12 ($P = 0.07$) and a negative association with Mode 15 ($P = 0.08$). Applying these deformation modes onto the template enabled us to visualize and quantify the shape changes. From *Figure 3*, we observed that in our population, PRVi is related to RV global enlargement (Mode 1), bulging of the outflow tract towards an aneurismal shape (Modes 12 and 15), dilatation of the RV apex (Modes 12 and 15), dilatation of the pulmonary valve annulus, and a more circular tricuspid valve. These findings are consistent with previous results on a different population.[15,22]

Table 2 Regression coefficients between the shape vectors and PRVi after model reduction ($R^2 = 0.39$, $P = 0.013$)

	Estimate	Std. error	*t*-value	*P*-value
(Intercept)	**34.7212651**	**2.2253078**	**15.603**	**3.14E-16**
Mode 1	**0.0025349**	**0.0009366**	**2.706**	**0.011**
Mode 2	0.0045411	0.0034199	1.328	0.1939
Mode 10	−0.0163286	0.0124469	−1.312	0.1992
Mode 12	**0.0264241**	**0.0142791**	**1.851**	**0.0738**
Mode 15	**−0.0394336**	**0.0221589**	**−1.78**	**0.085**
Mode 18	−0.0410802	0.0272007	−1.51	0.1411

Six modes were kept. The sign of the coefficients indicates the direction of correlation for increasing PRVi. In bold the modes that were relevant to PRVi.

Discussion

To the best of our knowledge, this study constitutes a first attempt to correlate 3D RV shape with clinical parameters in patients with rToF using computer modelling. We have shown in a realistic way that the RV dilates (the outlet bulges and the apex deforms) as PR volume worsens. Owing to the fact that our approach considers the complete 3D shape on a regional level, it could constitute a useful tool for the management of rToF patients by providing quantitative features of RV shape that are more discriminating compared with standard CMR analysis, which relies only on the volume.

Although our findings are relatively known and our work is similar to Sheehan *et al.*,[16] our approach is radically different and opens new avenues in the shape analysis of the cardiac chambers. While Sheehan *et al.* analysed specific lumped markers from the 3D shape, we assess the entire 3D shape analysed directly, without the introduction of any prior knowledge, which is implicitly the case when selecting specific metrics. As a result, we can now identify more subtle features that cannot be encoded by lumped metrics easily. The features related to PR are automatically extracted by the correlation analysis. It is, therefore, interesting to see that we can recover the main features of rToF using our approach.

Though RV volume is one of the outcome predictors in rToF patients, chamber geometry, myofibre architecture, RV compliance, chamber contraction pattern, and the interdependence between LV and RV function are likely to play a role in defining the long-term outcomes for rToF patients. In addition, any RV outflow tract patch and the consequent localized fibrosis and akinesis/dyskinesis of the RV outflow tract, which vary from patient to patient, may play a role in pathophysiology.[23] Assessment of the RV outflow tract remains difficult on both CMR and echo[24,25] and an overall 3D assessment of RV shape may prove to be a useful biomarker. The methods we describe could give us a more realistic and complete view of 3D RV shape, which may give further insight into the timing of PVR, though larger scale studies to assess the usefulness of such a new biomarker would need to be performed. Importantly, though our method has
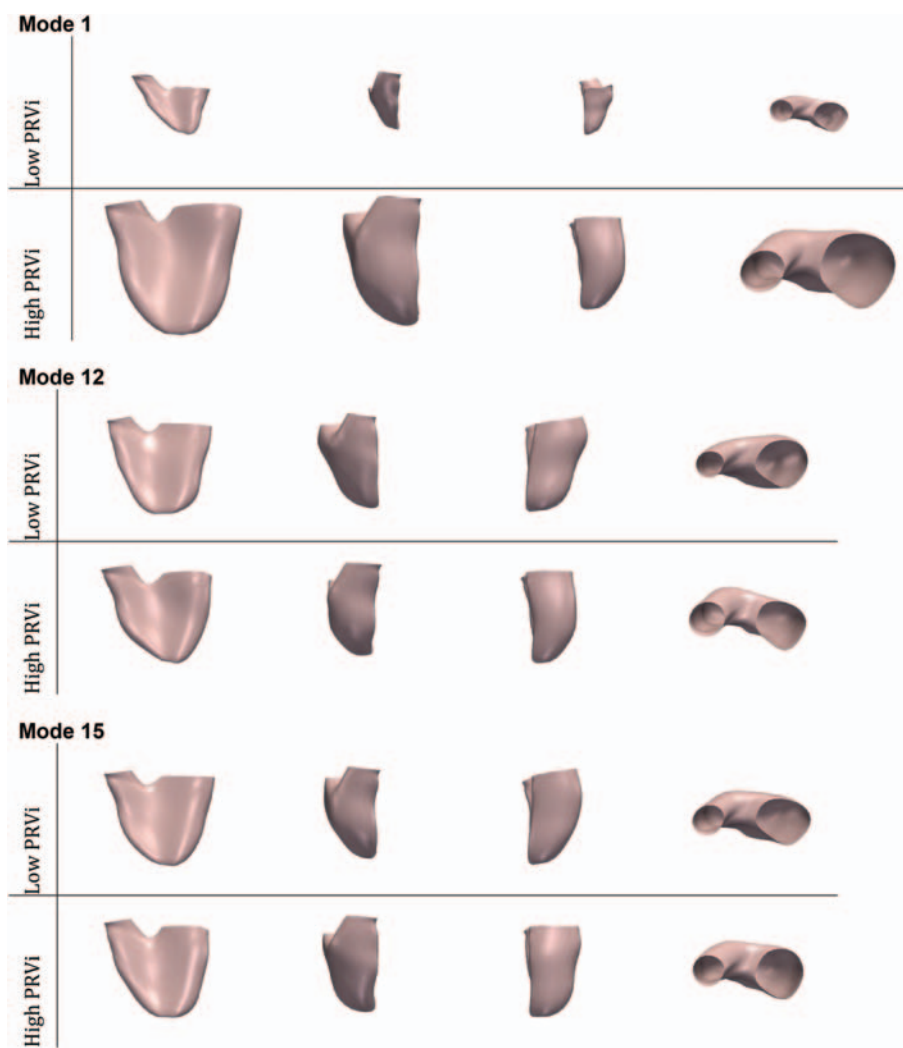
Figure 3 Variations in RV shape correlated with PRVi in 38 patients. Modes 1, 12, and 15 were found significantly related to PRVi.

been developed using CMR data, it could be applied to 3D echo data, to act as a surrogate for PR severity. As semi-automatic or fully automatic methods are available to segment the heart on echo images, the resulting meshes could then be directly used in our framework to extract shape features. Other functional parameters, such as Doppler flow metrics or strain could also be included in the statistical analysis for a more comprehensive correlation between shape and function.

Although there is strong evidence that PVR is safe and effective at eliminating or greatly reducing PR, it should be kept in mind that in the majority of studies global RV systolic function remains unchanged. Moreover, at present, data regarding the effects of PVR on arrhythmia propensity and objective exercise parameters are inconsistent. Therefore, having additional information may be useful for defining patient outcomes. In addition, our model can be useful to quantify the degree of bulging by computing the RV shape vector of a patient, an index that could be used as a predictor of PVR. Thus, it could be helpful not only to facilitate the

decision on the right timing and type of surgical approach, but also to monitor the effect of chronic PR and, consequently, the volume load on RV mechanics during the life of a specific rToF patient.

In the future, we could perform analysis with BSA, patient age[15] and gender[26] to understand how RV shape changes in relation to growth, and use such models to predict the PRV over time. Deviation from what is known to be the 'normal', predicted RV shape change for any given individual patient might alert us to subclinical deterioration in RV function that could trigger closer clinical follow-up or even early PVR. While patients who are doing better than expected may be able to have PVR deferred. Furthermore, analysis of the LV–RV interaction by directly applying our segmentation and shape methodology of the bi-ventricular myocardium could provide further novel information. Finally, our approach might also be applied on post-operative data to study the long-term impact of new PVR therapies on RV anatomy.[27,28]

Limitations

A drawback of this study is the lack of control subjects that, unfortunately, prevented us from studying the differences between rToF patients and healthy subjects, as in the study of Zhang *et al.*[29] Furthermore, we have analysed a relatively small number of patients to estimate the template, as CMR data were not available retrospectively in all patients recruited for the Health-e-Child study. Future work should include the analysis of a larger population to confirm our findings.

Conclusions

We have provided new insights into the mechanical adaptation of RV to chronic significant pulmonary insufficiency in rToF patients. The measurement of an RV shape biomarker may allow for personalized follow-up of rToF patient, which may help defining the timing of PVR.

References

1. Nollert G, Fischlein T, Bouterwek S, Böhmer C, Klinner W, Reichart B. Long-term survival in patients with repair of tetralogy of Fallot: 36-year follow-up of 490 survivors of the first year after surgical repair. *J Am Coll Cardiol* 1997;**30**:1374–83.
2. Gatzoulis MA, Balaji S, Webber SA, Siu SC, Hokanson JS, Poile C et al. Risk factors for arrhythmia and sudden cardiac death late after repair of tetralogy of Fallot: a multicentre study. *Lancet* 2000;**356**:975–81.
3. Geva T, Sandweiss BM, Gauvreau K, Lock JE, Powell AJ. Factors associated with impaired clinical status in long-term survivors of tetralogy of Fallot repair evaluated by magnetic resonance imaging. *J Am Coll Cardiol* 2004;**43**:1068–74.
4. Dos L, Dadashev A, Tanous D, Ferreira-González IJ, Haberer K, Siu SC et al. Pulmonary valve replacement in repaired tetralogy of Fallot: determinants of early postoperative adverse outcomes. *J Thorac Cardiovasc Surg* 2009;**138**:553–9.
5. Lurz P, Coats L, Khambadkone S, Nordmeyer J, Boudjemline Y, Schievano S et al. Percutaneous pulmonary valve implantation: impact of evolving technology and learning curve on clinical outcome. *Circulation* 2008;**117**:1964–72.
6. Geva T. Repaired tetralogy of Fallot: the roles of cardiovascular magnetic resonance in evaluating pathophysiology and for pulmonary valve replacement decision support. *J Cardiovasc Magn Reson* 2011;**13**:9.
7. Therrien J, Provost Y, Merchant N, Williams W, Colman J, Webb G. Optimal timing for pulmonary valve replacement in adults after tetralogy of Fallot repair. *Am J Cardiol* 2005;**95**:779–82.
8. Buechel ER, Dave HH, Kellenberger CJ, Dodge-Khatami A, Pretre R, Berger F et al. Remodelling of the right ventricle after early pulmonary valve replacement in children with repaired tetralogy of Fallot: assessment by cardiovascular magnetic resonance. *Eur Heart J* 2005;**26**:2721–7.
9. Oosterhof T, Meijboom FJ, Vliegen HW, Hazekamp MG, Zwinderman AH, Bouma BJ et al. Long-term follow-up of homograft function after pulmonary valve replacement in patients with tetralogy of Fallot. *Eur Heart J* 2006;**27**:1478–84.
10. Lee C, Kim YM, Lee CH, Kwak JG, Park CS, Song JY et al. Outcomes of pulmonary valve replacement in 170 patients with chronic pulmonary regurgitation after relief of right ventricular outflow tract obstruction: implications for optimal timing of pulmonary valve replacement. *J Am Coll Cardiol* 2012;**60**:1005–14.
11. Baumgartner H, Bonhoeffer P, De Groot NM, de Haan F, Deanfield JE, Galie N et al. ESC Guidelines for the management of grown-up congenital heart disease (new version 2010). *Eur Heart J* 2010;**31**:2915–57.
12. Hsia TY, Cosentino D, Corsini C, Pennati G, Dubini G, Migliavacca F. Modeling of congenital hearts alliance (MOCHA) investigators. Use of mathematical modeling to compare and predict hemodynamic effects between hybrid and surgical Norwood palliations for hypoplastic left heart syndrome. *Circulation* 2011;**124**(11 Suppl):S204–10.
13. Schievano S, Migliavacca F, Coats L, Khambadkone S, Carminati M, Wilson N et al. Planning of percutaneous pulmonary valve implantation based on rapid prototyping of the right ventricular outflow tract and pulmonary trunk from magnetic resonance imaging data. *Radiology* 2007;**242**:490–7.
14. Schievano S, Coats L, Migliavacca F, Norman W, Frigiola A, Deanfield J et al. Variations in right ventricular outflow tract morphology following repair of congenital heart disease—implications for percutaneous pulmonary valve implantation. *JCMR* 2007;**9**:687–95.
15. Mansi T, Voigt I, Leonardi B, Pennec X, Durrleman S, Sermesant M et al. A statistical model for quantification and prediction of cardiac remodeling: application to tetralogy of Fallot. *IEEE Trans Med Imaging* 2011;**30**:1605–16.
16. Sheehan FH, Ge S, Vick GW III, Urnes K, Kerwin WS, Bolson EL et al. Three-dimensional shape analysis of right ventricular remodeling in repaired tetralogy of Fallot. *Am J Cardiol* 2008;**101**:107–13.
17. Bodhey NK, Beerbaum P, Sarikouch S, Kropf S, Lange P, Berger F et al. Functional analysis of the components of the right ventricle in the setting of tetralogy of Fallot. *Circ Cardiovasc Imaging* 2008;**1**:141–7.
18. Zheng Y, Barbu A, Georgescu B, Scheuering M, Comaniciu D. Four-chamber heart modeling and automatic segmentation for 3-D cardiac CT volumes using marginal space learning and steerable features. *IEEE Trans Med Imaging* 2008;**27**:1668–81.
19. Arun KS, Huang TS, Blostein SD. Least-squares fitting of two 3-d point sets. *IEEE Trans Pattern Anal Mach Intell* 1987;**9**:698–700.
20. Durrleman S, Pennec X, Trouvé A, Ayache N. Statistical models of sets of curves and surfaces based on currents. *Med Image Anal* 2009;**13**:793–808.
21. Vaillant M, Glaunès J. Surface matching via currents. *Inf Process Med Imaging* 2005;**19**:381–92.
22. Mansi T, Durrleman S, Bernhardt B, Sermesant M, Delingette H, Voigt I et al. A statistical model of right ventricle in tetralogy of Fallot for prediction of remodeling and therapy planning. *Med Image Comput Comput Assist Interv* 2009;**12**(Pt 1):214–21.
23. Wald RM, Haber I, Wald R, Valente AM, Powell AJ, Geva T. Effects of regional dysfunction and late gadolinium enhancement on global right ventricular function and exercise capacity in patients with repaired tetralogy of Fallot. *Circulation* 2009;**119**:1370–7.
24. Kutty S, Zhou J, Gauvreau K, Trincado C, Powell AJ, Geva T. Regional dysfunction of the right ventricular outflow tract reduces the accuracy of Doppler tissue imaging assessment of global right ventricular systolic function in patients with repaired tetralogy of Fallot. *J Am Soc Echocardiogr* 2011;**24**:637–43.
25. Bonnemains L, Stos B, Vaugrenard T, Marie PY, Odille F, Boudjemline Y. Echocardiographic right ventricle longitudinal contraction indices cannot predict ejection fraction in post-operative Fallot children. *Eur J Echocardiogr* 2012;**13**:235–42.
26. Sarikouch S, Koerperich H, Dubowy KO, Boethig D, Boettler P, Mir TS et al. German Competence Network for Congenital Heart Defects Investigators. Impact of gender and age on cardiovascular function late after repair of tetralogy of Fallot. *Circ Cardiovasc Imaging* 2011;**4**:703–11.
27. Marianeschi SM, Santoro F, Ribera E, Catena E, Vignati G, Ghiselli S et al. Pulmonary valve implantation with the new shelhigh injectable stented pulmonic valve. *Ann Thorac Surg* 2008;**86**:1466–72.
28. Guccione P, Milanesi O, Hijazi ZM, Pongiglione G. Transcatheter pulmonary valve implantation in native pulmonary outflow tract using the Edwards SAPIEN™ transcatheter heart valve. *Eur J Cardiothorac Surg* 2012;**41**:1192–4.
29. Zhang H, Wahle A, Johnson RK, Scholz TD, Sonka M. 4-D cardiac MR image analysis: left and right ventricular morphology and function. *IEEE Trans Med Imaging* 2010;**29**:350–64.